

1 **Impact of the new Common Agricultural Policy of the EU on**
2 **the runoff production and soil moisture content in a**
3 **Mediterranean agricultural system**

4
5 **M. López-Vicente¹, A. Navas¹, L. Gaspar² and J. Machín¹**

6 [1]{Department of Soil and Water, Estación Experimental de Aula Dei, EEAD–CSIC. Avda.
7 Montañana 1005, 50059 Zaragoza, Spain }

8 [2]{Cranfield University, Cranfield Water Sciences Institute, Cranfield, Bedfordshire MK43
9 0AL, United Kingdom }

10 Correspondence to: M. López-Vicente (mvicente@eead.csic.es)

11

12 **Submitted: 7 April 2013**

13 **Accepted for publication in *Environmental Earth Sciences*: 2 September 2013 → DOI: [10.1007/s12665-013-2790-4](https://doi.org/10.1007/s12665-013-2790-4)**

14

15 **Abstract**

16 Soil moisture variability and the depth of water stored in the arable layer of the soil are
17 important topics in agricultural research and rangeland management. In this study we use the
18 Distributed Rainfall-Runoff (DR2) model to perform a detailed mapping of topsoil moisture
19 status (*SMS*) in a mountain Mediterranean catchment. This model, previously tested in the
20 same study area against the Palmer Z-index, is run at monthly scale for the current scenario of
21 land uses and under three scenarios that combine the land abandonment and the application of
22 the new Common Agricultural Policy (CAP) of the European Union. Under the current
23 conditions, runoff yield is scarce and presents a high spatial variability when monthly rainfall
24 intensity and depth are low, and infiltration processes mainly lead to water storage in the soil.
25 When rainfall intensity is high, runoff accumulation along the hillslopes controls the depth of
26 available water in the soil, and *SMS* is more homogeneous. On average, scrublands and
27 pasture have the wettest values, crops of winter cereal and abandoned fields have intermediate
28 conditions, and areas of bare soil and forest have the driest conditions all the year around. The
29 abandonment and no revegetation of the low productive fields located in steep areas and the

1 collapse of their landscape linear elements (LLEs) produces both an increase of 2.3% of the
2 overall *SMS* in the catchment in comparison with the current scenario but also an increment of
3 the effective runoff that cross the cultivated areas of the lowlands and the runoff depth that
4 reach the wetlands, increasing the soil erosion risk and compromising the conservation of the
5 lakes. When the new green areas of the CAP are installed in the upper part of the fields of the
6 lowlands and around the lakes, the runoff depth and thus siltation risk clearly decreases but
7 also *SMS* decreases 1.7 and 1.1% considering the current land uses and adding revegetation
8 practices in the abandoned fields, respectively. Hence, a management scenario where: i)
9 abandoned fields are covered with a dense cover of shrubs, ii) the LLEs are preserved, iii) the
10 green areas of the PAC are created, and iv) runoff harvesting practices are applied to partially
11 compensate the water deficit, will help to preserve the humidity of the soil and will be of
12 interest to keep the agricultural land use around the protected lakes of the study area.

13

14 **Keywords:** Topsoil moisture; DR2 model; winter cereal; Estaña Lakes; Mediterranean agro-
15 system; new Common Agricultural Policy

16

17 **1 Introduction**

18 Soil moisture monitoring and the study of its temporal and spatial variations are ongoing
19 trends in agricultural water research and rangeland management and restoration (e.g. Gao and
20 Shao, 2012; Gala and Melesse, 2012). In the last decade, the number of water balance models,
21 devices for the assessment of soil water content and drought indices has increased in all
22 scientific disciplines (e.g. Frot and van Wesemael, 2009; Vicente-Serrano et al., 2011a;
23 Mittelbach et al., 2012). Drought is one of the major natural hazards that trigger serious
24 economic and environmental damages. A direct and well documented correlation exists
25 between the available water storage in the entire soil profile and the crop yield in rain-fed
26 agricultural systems (Tao et al., 2003). This correlation is even more significant than that
27 between crop yield and rainfall depth or temperature. In the Iberian Peninsula, the mean
28 duration of drought episodes has increased in the last 3 decades by approximately 1 month
29 due to increases of the potential evapotranspiration rates (Vicente-Serrano et al., 2011b).

30 Large scale conversion of natural ecosystems to agricultural land has taken place in the last
31 three centuries exacerbating the problems of soil degradation (García-Ruiz, 2010). New

1 irrigated areas with an upward trend in water requirement are appearing as a consequence of
2 increasing world population (Neumann et al., 2011). The current global scenario of
3 agricultural expansion and climate change causes great stress on soil and water resources and
4 stress the need for research on sustainable agriculture (Yang et al., 2012). This concern has
5 promoted the creation of specific laws, such as the European Union Water Framework
6 Directive (DIRECTIVE 2000/60/EC) and the Thematic Strategy for Soil Protection (COM,
7 2006). The sustainable use of land resources is significant to keep economic development and
8 environmental protection in fragile agro-ecosystems where changes of land use and land
9 management are the main driving forces that modify the natural dynamic and rates of runoff,
10 soil moisture and sediment yield (Zhao et al., 2013). Recently the European Commission
11 presented a set of regulations that constitutes the draft of the new Common Agricultural
12 Policy (CAP) that will come into force in January 2014. The proposals of the new CAP
13 (http://ec.europa.eu/agriculture/cap-post-2013/legal-proposals/index_en.htm) set the rules for
14 a greener policy that will boost the efficiency of food production through better resource
15 management and farm innovation.

16 Accurate and realistic estimations of soil moisture and runoff require the use of many input
17 variables due to the spatial and temporal variability and complexity of the processes of runoff
18 generation and accumulation. Soil moisture maps can be drawn with data obtained from
19 satellite images, such as the information provided by SMOS (the European Space Agency's
20 Soil Moisture and Ocean Salinity mission; Piles et al., 2010) or by RADARSAT-1 SAR
21 (Synthetic Aperture Radar; Gala and Melesse, 2012) though the spatial resolution is usually
22 coarse for agricultural research. The collection of hydrological models include the empirical
23 ones, such as the "curve number model" (Soil Conservation Service, 1985), dynamic models
24 like LISEM (Sheikh et al., 2010) or KINEROS (Nedkov and Burkhard, 2012), regional scale
25 models such as the Soil Moisture Deficit Index (SMDI) and Evapotranspiration Deficit Index
26 (ETDI) (Narasimhan and Srinivasan, 2005), and event based runoff models from agricultural
27 fields and hillslopes (e.g. STREAM, Frot and van Wesemael, 2009). However, some of the
28 available rainfall-runoff models do not characterize the humidity status of the soil, such as the
29 CASC2D (Downer et al., 2002) and the TOPMODEL (Huang et al., 2012), or they are too
30 complex and require many input parameters, like the GSSHA (Gridded Surface/Subsurface
31 Hydrologic Analysis; Downer and Ogden, 2003) model. In this study, we run the water
32 balance DR2 model (López-Vicente and Navas, 2012) to perform a detailed mapping of
33 topsoil moisture, cumulative runoff and water deficit at monthly scale and under four different

1 scenarios of land uses that includes the strategies of the new CAP. In a previous study, the
2 DR2 model was tested in the same study area and for the current conditions against soil
3 moisture values of the Palmer Z-index, showing that the spatial predictions with the DR2
4 model identify the different sub-categories of soil wetness for each soil type in greater detail
5 than the Palmer Z-index (details in López-Vicente and Navas, 2012). This study provides
6 valuable information that will be of interest for developing a sustainable soil and water
7 resource management in both agricultural systems and rangelands. This target is achieved in a
8 medium size catchment located in the Spanish Pre-Pyrenees where rain-fed cultivated areas
9 are intersected with forest, scrublands and grass.

11 2 Materials and methods

12 2.1 Study area

13 The Estaña Lakes catchment is a medium-size watershed (246 ha) located in the External
14 Ranges of the Spanish Pre-Pyrenees and within the Ebro Basin (Fig. 1a). This study site
15 includes three fresh-water lakes with a maximum flooding area of 17.3 ha. The three lakes
16 and their surrounding vegetation cover 22.7 ha and are under regional protection since 1997.
17 The protected area is included in both the Inventory of Singular Wetlands of Aragón (BOA,
18 2010) and in the European NATURA 2000 network as Site of Community Importance (SCI).
19 Elevation ranges between 676 and 896 m a.s.l. and the mean slope steepness is 19.5%. Steep
20 slopes (slope steepness higher than 22.5%) occupy 20% of the study area whereas gentle
21 slopes (slope steepness lower than 8%) cover 33%. The parent material of the soils
22 corresponds to Mesozoic gypsiferous marls, dolomites, limestones, and sparse saline deposits
23 and karstic processes partially dominate the evolution of this landscape (López-Vicente et al.,
24 2009a). Twenty-one types of soils are distinguished using the FAO classification (Machín et
25 al., 2008) that can be grouped into six main types: Calcisols (covering 32% of the total
26 surface), Leptosols (32%), Regosols (23%), Gleysols (4%), Gypsisols (5%) and Vertisols
27 (3%). Calcisols and Leptosols are associated to limestones, and Gypsisols, Regosols and
28 Vertisols to clayish materials. Texture is mainly silty loam and in some parts silty clay loam.
29 Gleysols are developed on clay materials where the water table is seasonally near the soil
30 surface and appear around the lakes. The different soil types present a complex spatial
31 distribution as a consequence of the intricate geology and topography (Fig. 1b).

1 The study area has a relatively long history (since the 10th century) of human occupation like
2 the San Esteban romance hermitage from the 11th century, agricultural practices and water
3 management (Morellón et al., 2008), with increasing population along the 19th century and a
4 continuous depopulation trend since then (Morellón et al., 2011). Nowadays, there are only 8
5 citizens in the Estaña village and most farmers live in other next villages like Benabarre and
6 Estopiñán del Castillo. The landscape is representative of the typical former rain-fed
7 Mediterranean agro-ecosystem where small patches of natural and anthropogenic areas are
8 heterogeneously distributed (Fig. 1c). Cropland of winter barley, pasture and orchards cover
9 31% of the study area, whereas forest and scrubland occupy 67%. The remaining 2% of the
10 soil surface is covered with rock pavements and screes. These percentages are related to the
11 soil surface without considering the lakes. Active soil erosion by water affects large parts of
12 this study site such as it appears described in the literature (e.g. López-Vicente and Navas,
13 2010; Gaspar et al., 2013; Navas et al., 2013) with high rates of soil loss mainly affecting the
14 crops (ranging from almost zero to 108 Mg / ha yr) and areas with low vegetation cover and
15 also high rates of sedimentation are threatening the lakes (ca. 3.41 mm / yr) (Morellón et al.,
16 2011). These studies highlight that siltation processes seriously threaten the wetlands of the
17 Estaña Lakes and thus mitigation and conservation practices are urgently needed.

18 The study area is located between the semi-arid areas of the Ebro valley to the south and the
19 humid areas of the Pyrenees to the north. Climate is continental Mediterranean with two
20 humid periods, one in spring (April and May) and a second in autumn (September and
21 October) and a dry summer with rainfall events of high intensity. The average maximum
22 rainfall intensity in 30 min, $I_{30\max}$, is higher than 15 mm h⁻¹ between May and October,
23 **attaining the highest values, from 22 to 26 mm h⁻¹ in July, August and September, and below**
24 **10 mm h⁻¹ between December and March** (López-Vicente et al., 2008) (Fig. 1d). Average
25 annual precipitation at the weather station of Canelles (8 km to the southeast of the study
26 area) was 520 mm for the reference period 1961-1990 considered by the World
27 Meteorological Organization, whereas the average precipitation during the last teen years
28 (2002-2011) was 15% lower (442 mm) (Fig. 1e). Annual precipitation has a strong inter-
29 annual oscillation of 378% for the period 1941–2011. The average annual potential
30 evapotranspiration is 1227 mm at the Barbastro weather station (33 km to the west of the
31 study area) (Fig. 1f). Low summer precipitation can cause summer droughts and long periods
32 of low rainfall depth can cause severe damage in natural vegetation and crops, and reduce the
33 volume of available water in the lakes. From an average number of 83 annual rainfall events

1 in the Canelles station, only 11 had precipitation above 12.7 mm and can be considered as
2 erosive events (Fig. 1d) following the definition proposed by Renard et al. (1997). Weather,
3 topography, land uses and tillage practices in the study area are representative of rain-fed
4 areas in Mediterranean mountainous agro-ecosystems.

5 2.2 The DR2 model

6 The water balance Distributed Rainfall-Runoff (DR2) model estimates for each month of the
7 year the soil moisture status (*SMS*) of the arable layer of the soil at hillslope and catchment
8 scale. This model, developed by López-Vicente and Navas (2012) and enhanced by López-
9 Vicente et al. (2013a), was applied in the same study area to obtain a detailed analysis of the
10 different role played by the topographic, climatic and infiltration parameters on the soil
11 moisture status. These authors successfully validated the predictions of the DR2 model
12 against values of the widely used Palmer moisture anomaly index (*Z*-index; Palmer, 1965).
13 Even though, the predictions of the DR2 model describe with more detail the spatial and
14 temporal changes of *SMS* than the Palmer *Z*-index. In this study, the DR2 model is applied
15 with an extended database of climatic parameters and a more detailed map of the different soil
16 types and their infiltration values to assess the *SMS* changes under different land use
17 scenarios. The DR2 model computes the *SMS* as the ratio between the depth of actual
18 available water (W_{aa} , mm) and potential reference evapotranspiration (ET_0 , mm):

$$19 \quad SMS = \frac{W_{aa}}{ET_0}. \quad (1)$$

20 where W_{aa} is defined as the total depth of water that is stored and infiltrated in the soil profile
21 during an average storm event for each month. Water inputs are assumed to be the sum of the
22 direct rainfall depth and of the upslope contributing runoff, and moisture demand is computed
23 as equal to potential evapotranspiration. The depth of W_{aa} at each pixel of the study area is
24 computed with GIS techniques following a sequence of calculations in three steps such as it
25 appears in Fig. 2. In the first step the unsaturated and saturated pixels by direct rainfall (no
26 runoff contribution) are distinguished. In the second step unsaturated pixels with and without
27 upslope contribution of runoff are discriminated. Finally, the upslope contributing runoff is
28 calculated for the unsaturated and saturated pixels as a function of the effective depth of
29 cumulative runoff. Following this step-by-step approach five different situations of water
30 inflow in the soil are distinguished (Fig. 2).

1 2.2.1 Initial runoff generated at raster cell

2 Soil only becomes saturated during a storm event or when the water table reaches the soil
 3 surface. Time to ponding (T_p , s) is the time until the surface of the soil is saturated under a
 4 rainfall intensity greater than the saturated hydraulic conductivity (K_{fs} , cm s^{-1}) (Esteves et al.,
 5 2005). Before T_p all the water infiltrates, beyond T_p only a fraction goes into the soil profile
 6 and the other part becomes runoff. Time to ponding depends on soil infiltration properties,
 7 rainfall intensity and the antecedent soil moisture content and can be calculated as a function
 8 of saturated hydraulic conductivity (K_{fs} , cm s^{-1}) and soil sorptivity (S_p , $\text{cm s}^{-0.5}$). Hogarth et al.
 9 (1991) proposed that time to ponding (T_p , s) has a minimum and a maximum time and state
 10 that the average value can be calculated as:

$$11 \quad \frac{1}{2} \frac{S_p^2}{K_{fs}} \ln \left(\frac{I}{I - K_{fs}} \right) \leq T_p \leq \frac{1}{2} \frac{S_p^2}{I - K_{fs}}, \quad (2)$$

$$12 \quad S_p = \sqrt{2 \Delta \theta \phi}, \quad (3)$$

$$13 \quad \Delta \theta = \theta_s - \theta_0. \quad (4)$$

14 where I (cm s^{-1}) is the rainfall intensity, ϕ is the matrix flux potential ($\text{cm}^2 \text{s}^{-1}$) of each soil
 15 type and θ_s (% vol.) and θ_0 (% vol.) are the saturated and initial volumetric water content,
 16 respectively. The saturated volumetric water content is the maximum amount of water that
 17 can be stored within the soil and the initial water content is the volume directly measured in
 18 the field (antecedent topsoil moisture).

19 Time to ponding is calculated in each point of topsoil moisture measurement for a
 20 characteristic rainfall event for a month (i.e. average maximum intensity). Then, the potential
 21 overland flow per raster cell for each month m (Q_{0m} , mm) is estimated as a function of the
 22 depths of monthly effective rainfall (ER_m , mm) and rainfall to ponding (Rp_m , mm):

$$23 \quad Q_{0m} = ER_m - \left[Rp_m e_m \right] \geq ER_m - \left[Rp_m I_m e_m \right] 0, \quad (5)$$

$$24 \quad ER_m = R_m \left[1 - A_m \right] \cos S. \quad (6)$$

25 where Tp_m is the monthly time to ponding (s), I_m is the monthly rainfall intensity (cm s^{-1}) and
 26 e_m is the monthly number of rainfall events. Values of ER are estimated after considering the
 27 depth of precipitation intercepted by the canopy of the crops and natural vegetation, A (0–1),
 28 from the total rainfall depth, R (mm), and using the improvement presented by Morgan and

1 **Duzant (2008)** to consider the effect of slope angle, S (radians), on the quantity of rain
 2 received per unit area. The DR2 model runs on a monthly time step and intends to assess the
 3 average wetness status of the soil and not to calculate the humidity of the soil after each
 4 rainfall event.

5 **2.2.2 Effective runoff (CQ_{eff}) and actual available water (W_{aa})**

6 Once time to ponding and initial runoff are calculated at each sampling point, the
 7 corresponding maps for the whole catchment are created with the Kriging interpolation
 8 method (ordinary type with constant trend removal) that gets the minimum standard error. In
 9 the second step of the DR2 model, initial runoff is routed into the digital elevation model
 10 (DEM) of the catchment using the multiple flow accumulation algorithm with a coefficient of
 11 concentration of 0.9 and the potential cumulative runoff, CQ_0 (mm), is obtained. In this step
 12 the effect of the man-made linear landscape elements ($LLEs$) is added as effective players
 13 modifying the natural runoff connectivity along the hillslopes and fields. This concept is
 14 based on the index of connectivity (IC) presented by **Borselli et al. (2008)** and successfully
 15 used by these authors and by others (e.g. **López-Vicente et al., 2013b**; **Cavalli et al., 2013**) in
 16 medium-size agricultural and mountainous catchments in Italy and Spain to identify areas
 17 with net soil loss and deposition. The digital elevation model of the study area is very
 18 accurate allowing the precise spatially distributed simulation of the runoff processes. Maps of
 19 CQ_{0m} draw narrow overland flow pathways within the gullies and channels and wide
 20 pathways near the divides, in the interrill areas and in the gentle areas of the catchment.

$$21 \quad CQ_{0m} = f(Q_{0im}, \text{Acc. Algorithm}_{MD}^{c=0.9}, LLEs, DEM_{resol}). \quad (7)$$

22 As there are many types of cumulative algorithms, and each type generates a different map
 23 with different values, a water balance correction factor (α) is added to achieve that the volume
 24 of balanced potential cumulative runoff (CQ_{0B}) equals the initial volume of available water to
 25 be accumulated along the catchment. The “ α ” factor allows other users of the DR2 model to
 26 choose whatever type of cumulative algorithm and improves the parameterization of the
 27 model. Then, the effective cumulative runoff (CQ_{eff-m} , mm) is calculated after considering the
 28 saturated hydraulic conductivity (K_{fs} , mm s⁻¹) and the average duration of a storm after the
 29 soil becomes saturated till the end of the rainfall event for each month m (Tq_m , s):

$$1 \quad CQ_{0Bm} = \alpha \cdot CQ_{0m} = \frac{\sum_{i=1}^{i=k} ER_{im} - \sum_{i=1}^{i=k} Rp_{im} e_m}{\sum_{i=1}^{i=k} CQ_{0m}} \cdot CQ_{0m}, \quad (8)$$

$$2 \quad CQ_{eff-m} = CQ_{0Bm} - K_{fs} Tq_m e e_m - SS_{max-m} e e_m \sin S, \quad (9)$$

$$3 \quad Tq_m = (TER_m - Tp_m) + Tq_{AfER} = (TER_m - Tp_m) + (FIL/FIV), \quad (10)$$

4 and the maximum amount of water retained on the soil surface (SS_{max-m} , mm) according to
5 **Driessen (1986)**:

$$6 \quad SS_{max-m} = 0.5 RG_m \frac{\sin^2(SIG - S) \cot(SIG + S) + \cot(SIG - S)}{\sin(SIG) 2 \cos(SIG) \cos(S)}. \quad (11)$$

7 and the slope steepness (S , radians). Where TER_m (s) is the total duration of an average storm
8 event considering an average value of rainfall intensity for each month m , FIL (m) is the flow
9 length and FIV (m/s) is the flow velocity. RG_m (mm) is the surface roughness, i.e. the
10 maximum depth of the soil micro-relief, and SIG (radians) is the surface furrow and ridge
11 angle determined by tillage marks and micro-topography. A SIG value of 30° is used in the
12 study area according to the value used in the previous application of the *DR2* model. Finally,
13 values of actual available water (W_{aa}) and soil moisture status (SMS) are estimated for each
14 month following the comprehensive approach described in **Fig. 2** and Eq. (1). Values of SMS
15 are scaled so that they fit into seven categories (see **Table 1**).

16 **2.3 Land use scenarios and simulation of the new CAP of the EU**

17 The *DR2* model has been run under four different scenarios of land uses (**Fig. 3**). The first one
18 mirrors the current conditions of land uses and landscape management, whereas the other
19 scenarios represent three different possibilities of land uses and landscape management under
20 the imminent application of the new CAP of the EU and the trend of land use changes
21 observed in the last decades in Spanish Mediterranean agricultural systems. European
22 Commission plans to require farmers to set aside green areas under the next phase of the EU's
23 agriculture support programme. Farmers who get EU support would have to set aside 7% of
24 their land as wooded areas or habitats as part of the EU executive's draft proposals for a
25 greener Common Agricultural Policy (CAP) that will be considered over 2013.

1 Nowadays, fields of winter barley cover 28.6% of the study area, whereas pastures and
2 orchards only represent 2.2% and 0.5% of the total surface. The 28 recently abandoned fields,
3 less than 25 years ago, appear in the hillslopes and summarizes 4.0% of the total surface of
4 the study area. The 32 old abandoned fields, more than 50 years ago, occupy 10.5 ha (4.6% of
5 the total surface). Cultivated fields are on average only 0.62 ha and often trails adopt irregular
6 shapes. The current landscape linear elements have a total length of 19,800 meters and
7 include agricultural and step agricultural terraces, buffer strips, ditches, pond walls, small
8 settlements, scarps and screes.

9 In the first simulated scenario (SimSc1), crops located in steep areas are abandoned without
10 adding any support or conservation plan, and the landscape linear elements (LLEs) associated
11 to these fields (mainly stone-walls) are ruined. In the simulated scenario 2 (SimSc2) and the
12 simulated scenario 3 (SimSc3) the green areas of the CAP are added as new LLEs. These
13 elements are located in two places: i) around the lakes in those areas where the direct supply
14 of sediments from the hillslopes to the wetlands have the highest rates, and ii) in the upper
15 part of the fields located on the lowlands of the catchment where runoff from the gullies can
16 trigger high values of soil loss. The 16 new LLEs protecting the lakes (P. lakes) occupy 0.98
17 ha and the 17 new LLEs protecting the crops (P. crops) cover 0.73 ha. The new green areas
18 seek to reduce the siltation rates to the wetlands and to preserve the arable layer of the soil
19 against soil erosion processes. In the SimSc2 all fields are cultivated such as it happens in the
20 current scenario whereas in the SimSc3 we have considered the abandonment of the low
21 productive fields located on the hillslopes like in SimSc1 but preserving the LLEs of the
22 fields (Table 2). The land use associated with the green areas corresponds to a dense coverage
23 of shrubs that is the most successful type of vegetation used in revegetation of banks and
24 slopes against soil erosion under Mediterranean climate conditions (Bochet et al., 2010).

25 **2.4 Acquisition of inputs data**

26 The monthly rainfall depth (R), rainfall intensity (I) and number of effective rainy days (e),
27 were obtained from the records of the Canelles weather station registered every 15 minutes
28 during the period 1997-2011. Values of potential evapotranspiration (ET_0) were acquired from
29 the records of the Barbastro weather station. Soil sorptivity (S_p) was estimated with previously
30 calculated values of saturated water content (θ_s) and antecedent soil moisture (θ_0) in 236
31 measurement points in the same study area (details in López-Vicente and Navas, 2012) and
32 those of precipitation intercepted by the canopy of the crops and natural vegetation (A) from

1 the previous study of characterization of the vegetation by López-Vicente et al., 2008. López-
2 Vicente et al. (2009b) measured the highest values of θ_0 in autumn (53.2% vol.) and the
3 lowest in summer (32.1% vol.) showing a positive correlation with seasonal precipitation and
4 an inverse relationship with seasonal solar radiation. Steep northern slopes presented the
5 highest values of θ_0 in spring, summer and winter and topsoil moisture progressively
6 decreases from steep northern slopes to gentle slopes and from gentle slopes to steep southern
7 slopes, defining a topographical trend. Any topographical trend was observed in autumn when
8 values of θ_0 were very high within the whole catchment. In this study we used a high spatial
9 resolution map of soil types where 21 different units were distinguished, according to the
10 FAO classification. In each of these units three measurements of matrix flux potential (ϕ) and
11 saturated hydraulic conductivity (K_{fs}) were performed, and a realistic map of the infiltration
12 processes was obtained. These maps improve significantly the accuracy of the DR2 model to
13 estimate the monthly values of time to ponding in comparison with the previous application of
14 the model in the same study area. In this work the roughness value, RG_m of Eq. (11), for forest
15 areas (random roughness, $RG = 20.3$ mm) was taken from Renard et al. (1997). Tillage tools
16 produce random and orientated roughness. For the tillage direction perpendicular to the
17 contours, RG is the roughness immediately after tillage and before rainfall, and it is 32 mm
18 for the plough, 23 mm for the heavy cultivator and 18 mm for the disk-harrow (Gilley and
19 Finkner, 1991). For the tillage direction parallel to the contours, RG is the orientated surface
20 roughness, which can be considered to be equal to the initial tillage depth immediately after
21 tillage and before rainfall (250 mm for the plough, 150 mm for the heavy cultivator and 80
22 mm for the disk-harrow). All input values, the interpolation and mathematical operations and
23 the output maps were done with the ArcView[®] GIS 3.2 and ArcMap[™] 10.0 applications at a
24 spatial resolution of 5 x 5 m of cell size.

25

26 **3 Results and discussion**

27 **3.1 Current scenario**

28 On a monthly basis and on average for the whole catchment, predominant wet conditions
29 occurred during the period October–January and in a minor way in April, whereas a dry
30 situation appeared in the soils in June, July and August. Drying-up conditions were identified
31 in February and May and wetting-up conditions occurred in March and September (Fig. 4).

1 These temporal patterns were previously described by López-Vicente and Navas (2012) in the
2 same study area and also agreed with those described by Latron and Gallart (2008) in the
3 small Can Vila catchment (NE Spain), where climate and topographic conditions are
4 comparable to those in the Estaña Lakes catchment. In this study, the spatial prediction of
5 actual available water has been refined and the new maps of SMS draw with more detail the
6 spatial changes of soil moisture. As it was studied by Rojas et al. (2008) in soil erosion
7 models and by Xu et al. (2007) in a rainfall-runoff model, the spatial resolution of the input
8 maps affects the ability of predicting models to produce accurate and realistic maps.
9 Therefore, the enhanced maps of W_{aa} and SMS obtained in this study let us refine the analysis
10 of the soil moisture variations for the different land uses and also to obtain an accurate
11 prediction of the effect of the three simulated scenarios on SMS changes.

12 Under the current scenario (year 2013), from November to June (8 months) areas with no
13 runoff production appear due to the low values of rainfall intensity and the spatial variability
14 of Q_0 values is high. These conditions appear in an area of ca. 9% of the total soil surface
15 from November to March, of 3% in April and below 1% in May and June. The spatial
16 location of the areas with no runoff production is positively correlated with the presence of
17 soils with high infiltration rates (e.g. above 153 mm day^{-1} for the prevalent conditions of
18 rainfall intensity in December) and their extension decreases throughout these 8 months as
19 rainfall intensity increases. Moreover, from October to April (7 months) relatively large areas
20 of dry conditions, ca. 22% of the total soil surface, appear along the divides of the different
21 sub-catchments despite the overall wet conditions (average SMS > 1.1) described for the
22 whole catchment. This fact is explained by the low production of effective runoff (CQ_{eff})
23 during this period as a consequence of the concurrence of low rainfall intensity and relatively
24 high infiltration rates that present an average and maximum values of 153 and 434 mm day^{-1}
25 for the different soil types. According to Eq. (9) the infiltration rates and the number and
26 duration of the erosive events play a critical role in the estimation of the effective cumulative
27 runoff. Thus we consider that further research may include a detailed study of the combined
28 effect of soil types and land uses in the runoff production at hillslope and plot scales. Similar
29 spatial variations in runoff yields were described by Needelman et al. (2004) after analysis of
30 runoff depth in different types of soil with different infiltration rates. When rainfall intensity
31 (I) is high (July, August, September and October), Q_0 is predicted along the whole surface of
32 the catchment and when high values of I are combined with high values of rainfall depth

1 (from May to September), the variability of *SMS* is very low and produces homogeneous
2 patterns of the soil moisture status.

3 The soil moisture status varies for the main land uses of the Estaña Lakes catchment and these
4 variations also change during the twelve months of the year (Fig. 5). On average, scrublands
5 present the wettest values (annual value of *SMS* = 1.7) although pasture has the moistest
6 conditions in January, March and December (annual value of 1.6). Crops of winter cereal and
7 abandoned fields have similar conditions, with average values of 1.4 and 1.3, respectively,
8 whereas areas of bare soil (annual value of 1.2) and forest (annual value of 1.1) have the driest
9 conditions during all the year. The Fisher's least significant difference procedure denotes that
10 the differences are not statistically significant due to the low range of variation in the values
11 of *SMS*. A deeper and further analysis of the *SMS* as a function of the different land uses may
12 include the values of actual evapotranspiration instead of the currently used values of
13 potential reference evapotranspiration that offer and homogeneous map for each month. The
14 low values of *SMS* in the forestry soils are explained by the spatial location of the forests,
15 mainly placed on the divides of the catchment and along the divides of the different sub-
16 catchments, where runoff production is lower than the runoff depth generated on the
17 hillslopes and at the bottom of the catchment. Although the lowest standard deviations of *SMS*
18 for each land use appear from May to September, during the period from April to October, the
19 differences between the driest and wettest mean conditions among the different land uses are
20 the highest: forest soils are 41% drier than the scrubland soils during this period and 33%
21 drier from November to March in comparison with the scrubland and pasture soils. The
22 spatial variability of *SMS* obtained in this study as a function of the land use agree with other
23 studies performed in Mediterranean areas, such as in Greece (Kargas et al., 2012) where
24 plowed soils and land uses with high values of soil roughness store more water within the soil
25 profile. In a comparison study of the hydrologic response between two Spanish Pyrenean
26 catchments, one used for agriculture in the past, and the other covered by dense natural forest,
27 Lana-Renault et al. (2011) obtained similar spatial and temporal variations of soil moisture,
28 showing a marked seasonal pattern, with higher values of runoff in the agricultural catchment
29 under dry conditions, and usually higher values in the forested catchment under wet
30 conditions. We can summarize that the more water is available for the whole catchment, the
31 less difference appears between the different land uses though the variability of the *SMS*
32 within each land use increases.

1 3.2 Simulated scenarios

2 The abandonment of the low productive fields located in the steep slopes (1 year cultivated –
3 1 year fallow rotation) and the creation of new green areas significantly modifies the values
4 and spatial patterns of the effective cumulative runoff (CQ_{eff}). On an average monthly scale,
5 these changes can be observed in detail in Fig. 6. As can be seen in this figure, the collapse of
6 the stone-walls in SimSc1 trigger higher connectivity between the runoff pathways that cross
7 the abandoned fields, reducing the number of areas where runoff is blocked (Fig. 6, graphs
8 a.2, a.3 and a.4). Under this scenario, there is an increase of 30% of the depth of available
9 runoff that can be redistributed along the hillslope triggering the saturation of a larger area
10 than the area saturated in the current scenario (Fig. 6, graphs a.1 and a.5). However, when the
11 same fields are abandoned in SimSc3 and the LLEs are preserved, no significant change is
12 observed in the spatial patterns either the runoff depth or the CQ_{eff} on the hillslope and on the
13 set-aside fields. The conversion of small parts of the fields (0.84 ha, 1.1% of the original
14 cultivated area) and forest (0.87 ha, 0.6% of the original forestry area) into “green areas” in
15 SimSc2 and SimSc3 clearly modify the current spatial patterns and depth of cumulative
16 runoff along these new LLEs. This effect is observed both in the green areas bordering the
17 fields at the bottom of the catchment (Fig. 6, graphs b.1 and b.2) and in the green areas that
18 surround the lakes (Fig. 6, graphs c.1 and c.2). The new spatial patterns of CQ_{eff} shown in the
19 maps describe the existence of new areas where runoff is stopped preventing the continuity of
20 the overland flow pathways that currently reach the wetlands. The runoff-blocking-effect of
21 the new “green areas” will reduce the sediment yield into the lakes as there is a clear and
22 well-known relationship between the runoff depth and the amount of suspended sediments
23 delivered on (e.g. Onderka et al., 2012) and thus it will be of interest to preserve the wetlands
24 of the Estaña Lakes catchment.

25 On a monthly average basis and in comparison with the current conditions of humidity, the
26 soil moisture status changes 2.3% to wetter conditions in the SimSc1 for the whole catchment,
27 whereas drier conditions are predicted in SimSc2 (1.7% drier) and SimSc3 (1.1% drier) (Fig.
28 7). These changes are not constant during the whole year and significant variations are
29 observed for the different months. As can be seen in Fig. 8 between December and March the
30 humidity status of the soil changes to significant wetter conditions in SimSc1 (3.4% wetter)
31 and changes to drier conditions, 2.0 and 1.6%, in SimSc2 and SimSc3, respectively. However,
32 during the summer months these changes vary notably for SimSc1 and SimSc3 and opposite

1 conditions of humidity are found in comparison with the current scenario. From July to
2 September, drier conditions (0.2% on average) are obtained for the whole catchment in
3 SimSc1 and the general trend of drier conditions described for SimSc2 are only 0.5% on
4 average drier during these three months. From May to October wetter conditions of 0.5% on
5 average and by 0.9% in July and August are predicted for SimSc3, which disagree with the
6 yearly average change to drier conditions. This change of trend turned out to be of benefit for
7 the vegetation as the soil remains more humid than under the current scenario during the six
8 months period when temperatures and evapotranspiration are higher, and thus a lower water
9 stress of the vegetation can be expected. These variations are explained by the spatial location
10 of the landscape linear elements along the hillslopes and by the different processes of soil
11 saturation and runoff generation that take place during the different months with different
12 values of rainfall depth and intensity: saturation-excess overland flow during the winter
13 months and infiltration-excess overland flow in summer and autumn and partially in spring.
14 From July to October the whole soil surface of the Estaña Lakes catchment becomes saturated
15 for an average storm event (Q_0 of Eq. (5) is higher than zero) due to the high values of rainfall
16 intensity and thus the spatial pattern of generated runoff differ from those patterns and values
17 found during the rest of the year. In the current scenario the average runoff depth generated
18 per raster cell, Q_0 , equals 16, 23, 52 and 65 mm in July, August, September and October,
19 respectively, with minimum values of 14, 21, 50 and 59 mm. However, the high values of ET_0
20 registered in summer explain the dry conditions of the soils showed in Fig. 4. The evaluation
21 of these results against the intra-annual wet and dry periods described above for the current
22 scenario (standard deviation of the average monthly values of SMS equals 1.21) suggests that
23 the temporal changes that take place for SimSc2 ($sd = 1.18$) and SimSc3 ($sd = 1.19$) are
24 minor. Additionally, in the SimSc3 it takes place a lower increase of the soil humidity during
25 the wet period but also a lower decrease of the actual available water during the so-called
26 “extended summer period”, from May to October.

27 On annual basis, in the set-aside fields, the soil moisture status lightly changes to wetter
28 conditions (the average SMS decreases 0.1%) for SimSc1 and clearly changes to wetter
29 conditions (the average SMS decreases 9.5%) for SimSc3. The latest increase of humidity is
30 directly related to the higher values of soil roughness, RG in Eq. (11), of the coverage of
31 dense scrubland ($RG = 20.3$ mm) than the value of RG ascribed to the cultivated areas
32 (average $RG = 17.8$ mm). The first value agrees with the overall trend observed for the whole
33 catchment, whereas the value estimated for SimSc3 differs with the general trend observed for

1 the rest of the catchment and clearly supports the human-induced reforestation of the set-aside
2 fields as a clear increase of water storage is predicted. On the other hand, the set of green
3 areas protecting the fields located on the lowlands satisfactorily reduce the depth of water that
4 might cross through the new *LLEs* and reach the crops and thus a decrease in the intensity of
5 soil erosion could be expected. However, the clear decrease of 38% of the humidity status
6 predicted in the first row of pixels downwards the new green areas compromises the growth
7 and maintenance of the rain-fed crops. In order to supply fresh water to the field and thus to
8 compensate for the water deficit, we consider that runoff harvesting practices could be applied
9 in the new green areas protecting the crops. This technique has been successfully used in
10 other Mediterranean areas to address the scarcity of surface water, such as in Israel for crop
11 irrigation (Tal, 2006) and in California as a part of the water balance system of highly
12 anthropized areas (Strecker and Poresky, 2010). The green areas located around the three
13 wetlands of the study site show a decrease of 11.5% in the soil moisture status as a
14 consequence of the “runoff-blocking-effect” of these new *LLEs*. As the water table is near the
15 soil surface around the lakes, we do not expect water stress in the reed grass bordering the
16 lakes and thus the protecting effect of the new *LLEs* in the lakes would not compromise the
17 development of the natural vegetation.

18

19 **4 Conclusions**

20 Under the current conditions, runoff yield is scarce and presents a high spatial variability
21 when monthly rainfall intensity and depth are low, and infiltration processes lead to storage of
22 water in the soil. However, when rainfall intensity and/or depth is high, runoff accumulation
23 processes control the depth of water available in the soil, and the soil moisture status is more
24 homogeneous across the catchment. As the DR2 model calculates the *SMS* for each month
25 without considering the humidity status of the soil during the previous month or months,
26 some errors can happen and thus in further research a “memory factor” should be added to the
27 model of at least one month prior to refine the estimation of the classes of humidity.

28 As the application of the new CAP of the European Commission will be mandatory since
29 January 2014, and if the abandonment of the low productive fields would happen in few
30 years, we conclude that the SimSc3 summarizes the most-probably scenario of land uses and
31 management practices that might occur in the Estaña Lakes catchment. Although a low
32 decrease in the soil moisture status is predicted for the whole catchment in this scenario, a

1 clear increase of the humidity status of the soil is predicted for the set-aside fields revegetated
2 with a dense coverage of shrubs. In addition, the new green areas would create a runoff-
3 blocking-effect that will protect the fields located on the lowlands against the processes of soil
4 loss by water and will reduce the sediment yield to the wetlands. Therefore, the application of
5 the new CAP will be of interest to preserve the Estaña Lakes. As the new landscape linear
6 elements will reduce the runoff depth that reach the fields and thus the *SMS* would decrease in
7 a small section of the crops, we propose for future research the study and application of runoff
8 harvesting techniques along hillslopes in order to supply additional fresh water to the crops.
9 In order to spread the use of the DR2 model we are currently developing a module for the
10 open-source and free *SAGA* GIS software that is called *DR2-2013*[©] *SAGA v1.0*. This module
11 is built using C++ code and contains all scientific methods and equations, and is presented in
12 a user-friendly interface that will be of interest for the scientific and academic community as
13 well as for the European Authorities. The new module will offer 15 different options to model
14 runoff accumulation by using 8 different flow accumulation algorithms and will be available
15 in the web site of our research center (www.eead.csic.es) and also in the repository of the
16 Spanish Council for Scientific Research (<https://digital.csic.es/>) in autumn 2013.

17

18 **Acknowledgements**

19 This research was funded by the Projects “Erosion and redistribution of soils and nutrients in
20 Mediterranean agroecosystems: radioisotopic tracers of sources and sinks and modelling of
21 scenarios (EROMED) (CGL2011-25486/BTE)” of the Spanish Ministry of Economy and
22 Competitiveness (former Ministry of Science and Innovation) and “Mitigation of siltation of
23 the Estaña Lakes Wetlands (Huesca, Spain) under different scenarios of climate change: soil
24 and water trapping effectiveness of the “green areas” of the new CAP (Expedient number
25 2012 GA LC 034)” of the Regional Government of Aragón (Spain) and *Obra Social “la*
26 *Caixa”*.

27

1 **References**

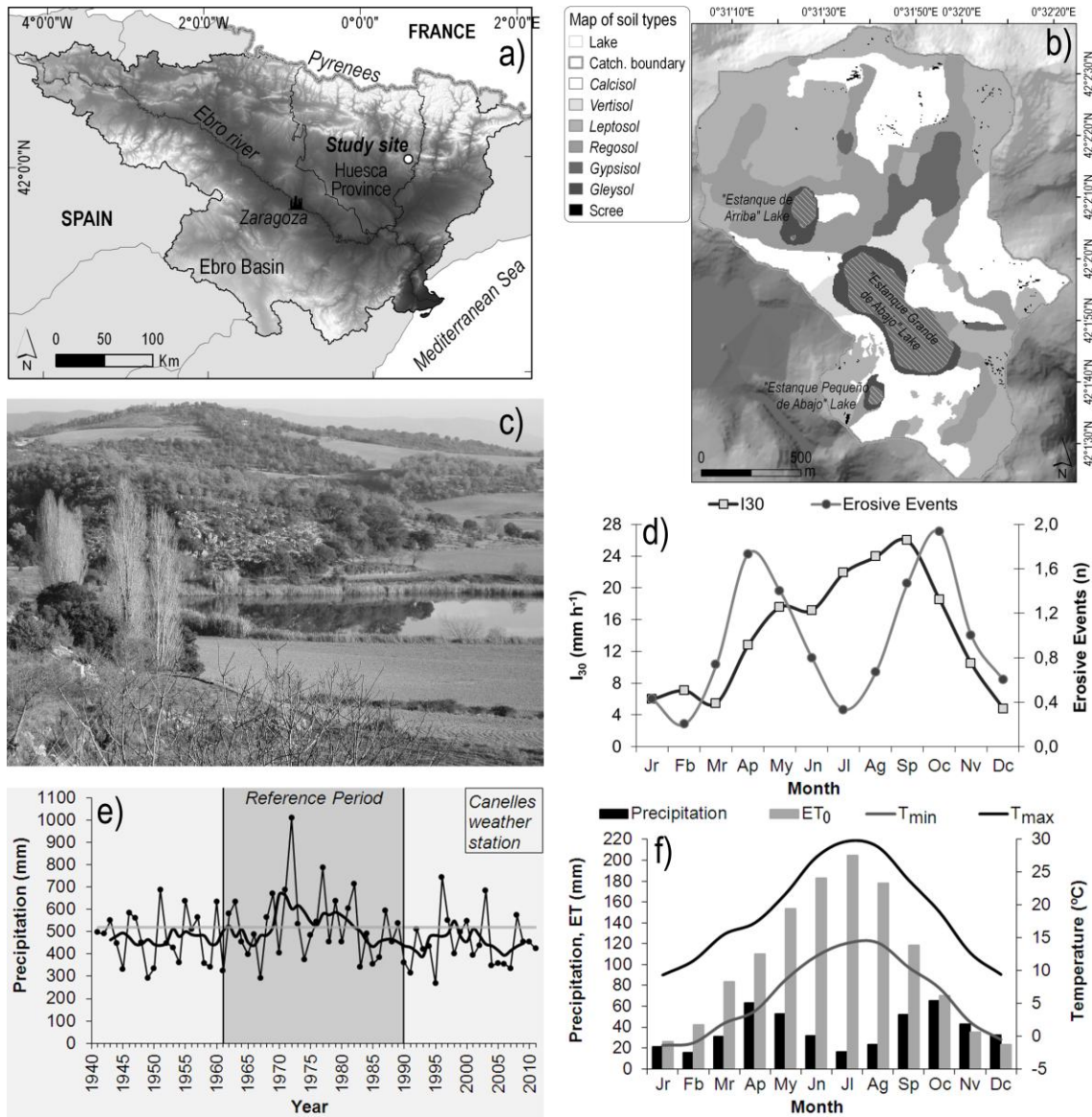
- 2 BOA (2010) DECRETO 204/2010, de 2 de noviembre, del Gobierno de Aragón, por el que se crea el Inventario
3 de Humedales Singulares de Aragón y se establece su régimen de protección. Boletín Oficial de Aragón,
4 Núm. 220, 11/11/2010, 25386–25400.
- 5 Bochet, E., García-Fayos, P., and Tormo, J (2010) How can we control erosion of roadslopes in semiarid
6 mediterranean areas? soil improvement and native plant establishment. *Land Degradation and Development*,
7 21(2), 110–121.
- 8 Borselli L, Cassi P, Torri D (2008) Prolegomena to sediment and flow connectivity in the landscape: A GIS and
9 field numerical assessment. *Catena* 75(3): 268-277.
- 10 Cavalli M, Trevisani S, Comiti F, Marchi L (2013) Geomorphometric assessment of spatial sediment
11 connectivity in small Alpine catchments. *Geomorphology* 188: 31-41.
- 12 COM - COMMISSION OF THE EUROPEAN COMMUNITIES (2006) Thematic Strategy for Soil Protection.
13 Communication from the Commission to the Council, the European Parliament, the European Economic and
14 Social Committee and the Committee of the Regions. Brussels, 22.9.2006. COM(2006)231 final.
- 15 DIRECTIVE 2000/60/EC OF THE EUROPEAN PARLIAMENT AND OF THE COUNCIL of 23 October 2000
16 establishing a framework for Community action in the field of water policy. Official Journal of the European
17 Communities L 327/1-72, 2000.
- 18 Downer, C.W. and Ogden, F.L. (2003) Prediction of runoff and soil moistures at the watershed scale: Effects of
19 model complexity and parameter assignment. *Water Resources Research* 39(3), SWC11–SWC113.
- 20 Downer, C.W., Ogden, F.L., Martin, W.D. and Harmon, R.S.: Theory, development, and applicability of the
21 surface water hydrologic model CASC2D. *Hydrological Processes*, 16(2), 255–275, 2002.
- 22 Driessen, P.M.: The water balance of soil. In: van Keulen, H., Wolf, J. (Eds.), *Modeling of Agricultural*
23 *Production: Weather, Soils and Crops*. Pudoc, Wageningen, The Netherlands, pp. 76–116, 1986.
- 24 Esteves, M., Descroix, L., Mathys, N., and Lapetite, J.M.: Soil hydraulic properties in a marly gully catchment
25 (Draix, France). *Catena*, 63(2-3), 282–298, 2005.
- 26 Frot, E. and van Wesemael, B.: Predicting runoff from semi-arid hillslopes as source areas for water harvesting
27 in the Sierra de Gador, southeast Spain. *Catena*, 79(1), 83–92, 2009.
- 28 Gala, T.S. and Melesse, A.M.: Monitoring prairie wet area with an integrated LANDSAT ETM+, RADARSAT-
29 1 SAR and ancillary data from LIDAR. *Catena*, 95, 12–23, 2012.
- 30 Gao, L. and Shao, M.: Temporal stability of soil water storage in diverse soil layers. *Catena*, 95, 24–32, 2012.
- 31 García-Ruiz, J.M.: The effects of land uses on soil erosion in Spain: A review. *Catena*, 81(1), 1–11, 2010.
- 32 Gaspar, L., Navas, A., Walling, D.E., Machín, J., and Gómez Arozamena, J.: Using ^{137}Cs and $^{210}\text{Pb}_{\text{ex}}$ to assess
33 soil redistribution on slopes at different temporal scales. *Catena*, 102, 46–54, 2013.

- 1 Gilley, J.E. and Finkner, S.C.: Hydraulic Roughness Coefficients as Affected by Random Roughness.
2 Transactions of the ASAE, 34(3), 897–903, 1991.
- 3 Hogarth, W.L., Sardana, V., Watson, K.K., Sander, G.C., Parlange, J.Y., and Haverkamp, R.: Testing of
4 approximate expression for soil water status at the surface during infiltration. Water Resources Research,
5 27(8), 1957–1961, 1991.
- 6 Huang, J.-C., Lee, T.-Y., Kao, S.-J., Hsu, S.-C., Lin, H.-J., and Peng, T.-R.: Land use effect and hydrological
7 control on nitrate yield in subtropical mountainous watersheds. Hydrology and Earth System Sciences, 16(3),
8 699–714, 2012.
- 9 Kargas, G., Kerkides, P., and Poulouvassilis, A.: Infiltration of rain water in semi-arid areas under three land
10 surface treatments. Soil and Tillage Research, 120, 15–24, 2012.
- 11 Lana-Renault, N., Latron, J., Karssenber, D., Serrano-Muela, P., Regüés, D., and Bierkens, M.F.P.: Differences
12 in stream flow in relation to changes in land cover: A comparative study in two sub-Mediterranean mountain
13 catchments. Journal of Hydrology, 411(3-4), 366–378, 2011.
- 14 Latron, J. and Gallart, F.: Runoff generation processes in a small Mediterranean research catchment (Vallcebre,
15 Eastern Pyrenees). Journal of Hydrology, 358(3-4), 206–220, 2008.
- 16 López-Vicente, M. and Navas, A. (2010) Relating soil erosion and sediment yield to geomorphic features and
17 erosion processes at the catchment scale in the Spanish Pre-Pyrenees. Environmental Earth Sciences, 61(1),
18 143–158.
- 19 López-Vicente, M. and Navas, A. (2012) A new distributed rainfall-runoff model (DR2) based on soil saturation
20 and runoff cumulative processes. Agricultural Water Management, 104, 128–141.
- 21 López-Vicente, M., Navas, A., and Machín, J. (2008) Identifying erosive periods by using RUSLE factors in
22 mountain fields of the Central Spanish Pyrenees. Hydrology and Earth System Sciences, 12(2), 523–535.
- 23 López-Vicente, M., Navas, A., and Machín, J. (2009a) Geomorphic mapping in endorheic catchments in the
24 Spanish Pyrenees: An integrated GIS analysis of karstic features. Geomorphology, 111(1-2), 38–47.
- 25 López-Vicente, M., Navas, A., and Machín, J. (2009b) Effect of physiographic conditions on the spatial variation
26 of seasonal topsoil moisture in Mediterranean soils. Australian Journal of Soil Research, 47(5), 498–507.
- 27 López-Vicente M, Navas A, Gaspar L, Machín J (2013a) Advanced modelling of runoff and soil redistribution
28 for agricultural systems: The SERT model. Agricultural Water Management 125: 1-12.
- 29 López-Vicente M, Poesen J, Navas A, Gaspar L (2013b) Predicting runoff and sediment connectivity and soil
30 erosion by water for different land use scenarios in the Spanish Pre-Pyrenees. Catena 102: 62-73.
- 31 Machín, J., López-Vicente, M., and Navas, A. (2008) Cartografía digital de suelos de la Cuenca de Estaña
32 (Prepirineo Central). In: Trabajos de Geomorfología en España, 2006-2008 (Benavente, J., Gracia, F.J.,
33 Eds.). SEG, Cádiz, Spain, pp. 481–484.
- 34 Mittelbach, H., Lehner, I., and Seneviratne, S.I.: Comparison of four soil moisture sensor types under field
35 conditions in Switzerland. Journal of Hydrology, 430-431, 39–49, 2012.

- 1 Morellón, M., Valero-Garcés, B., González-Sampériz, P., Vegas-Vilarrúbia, T., Rubio, E., Rieradevall, M.,
2 Delgado-Huertas, A., Mata, P., Romero, O., Engstrom, D.R., López-Vicente, M., Navas, A., and Soto, J.:
3 Climate changes and human activities recorded in the sediments of Lake Estanya (NE Spain) during the
4 Medieval Warm Period and Little Ice Age. *Journal of Paleolimnology*, 46(3), 423–452, 2011.
- 5 Morellón, M., Valero-Garcés, B., Moreno, A., González-Sampériz, P., Mata, P., Romero, O., Maestro, M., and
6 Navas, A.: Holocene palaeohydrology and climate variability in northeastern Spain: The sedimentary record
7 of Lake Estanya (Pre-Pyrenean range). *Quaternary International*, 181, 15–31, 2008.
- 8 Morgan, R.P.C. and Duzant, J.H.: Modified MMF (Morgan-Morgan-Finney) model for evaluating effects of
9 crops and vegetation cover on soil erosion. *Earth Surface Processes and Landforms*, 33(1), 90–106, 2008.
- 10 Narasimhan B. and Srinivasan, R.: Development and evaluation of Soil Moisture Deficit Index (SMDI) and
11 Evapotranspiration Deficit Index (ETDI) for agricultural drought monitoring. *Agricultural and Forest
12 Meteorology*, 133(1-4), 69–88, 2005.
- 13 Navas, A., López-Vicente, M., Gaspar, L., and Machín, J.: Assessing soil redistribution in a complex karst
14 catchment using fallout ¹³⁷Cs and GIS. *Geomorphology*, 196, 231–241, 2013.
- 15 Nedkov, S. and Burkhard, B.: Flood regulating ecosystem services—Mapping supply and demand, in the
16 Etropole municipality, Bulgaria. *Ecological Indicators*, 21, 67–79, 2012.
- 17 Needelman, B.A., Gburek, W.J., Petersen, G.W., Sharpley, A.N., and Kleinman, P.J.A.: Surface Runoff along
18 Two Agricultural Hillslopes with Contrasting Soils. *Soil Science Society of America Journal*, 68, 914–923,
19 2004.
- 20 Neumann, K., Stehfest, E., Verburg, P.H., Siebert, S., Müller, C., and Veldkamp, T.: Exploring global irrigation
21 patterns: A multilevel modelling approach. *Agricultural Systems*, 104(9), 703–713, 2011.
- 22 Onderka, M., Krein, A., Wrede, S., Martínez-Carreras, N., and Hoffmann, L.: Dynamics of storm-driven
23 suspended sediments in a headwater catchment described by multivariable modeling. *Journal of Soils and
24 Sediments*, 12(4), 620–635, 2012.
- 25 Palmer, W.C.: Meteorological drought. Office of Climatology, research paper no. 45, U.S. Weather Bureau, 58,
26 1965.
- 27 Piles, M., Camps, A., Vall-llossera, M., Monerris, A., Talone, M., and Sabater, J.M.: Performance of soil
28 moisture retrieval algorithms using multiangular L band brightness temperatures. *Water Resources Research*,
29 46, W06506, 2010.
- 30 Renard, K.G., Foster, G.R., Weesies, G.A., McCool, D.K., and Yoder, D.C.: Predicting Soil Erosion by Water:
31 A Guide to Conservation Planning with the Revised Universal Soil Loss Equation (RUSLE). Handbook
32 #703. US Department of Agriculture, Washington, DC, 1997.
- 33 Rojas, R., Velleux, M., Julien, P.Y., and Johnson, B.E.: Grid scale effects on watershed soil erosion models.
34 *Journal of Hydrologic Engineering*, 13(9), 793–802, 2008.

- 1 Sheikh, V., van Loon, E., Hessel, R., and Jetten, V. (2010) Sensitivity of LISEM predicted catchment discharge
2 to initial soil moisture content of soil profile. *Journal of Hydrology*, 393(3-4), 174–185.
- 3 Soil Conservation Service, USDA (1985) *Hydrology, National engineering handbook, Supplement A, Sect. 4,*
4 *Chapter 10.* USDA, Washington, D.C.
- 5 Strecker, E. and Poresky, A.: The feasibility and desirability of stormwater retention on site in California and on
6 the west coast. In: *Low Impact Development 2010: Redefining Water in the City - Proceedings of the 2010*
7 *International Low Impact Development Conference, San Francisco, California, pp. 1022–1035, 2010.*
- 8 Tal, A.: Seeking sustainability: Israel's evolving water management strategy. *Science*, 313(5790), 1081–1084,
9 2006.
- 10 Tao, F., Yokozawa, M., Hayashi, Y., and Lin., E.: Changes in agricultural water demands and soil moisture in
11 China over the last half-century and their effects on agricultural production. *Agricultural and Forest*
12 *Meteorology*, 118(3-4), 251–261, 2003.
- 13 Vicente-Serrano, S.M., López-Moreno, J.I., Gimeno, L., Nieto, R., Morán-Tejeda, E., Lorenzo-Lacruz, J.,
14 Beguería, S., and Azorin-Molina, C.: A multiscale global evaluation of the impact of ENSO on droughts.
15 *Journal of Geophysical Research D: Atmospheres*, 116(20), Article number D20109, 2011a.
- 16 Vicente-Serrano, S.M., López-Moreno, J.I., Drumond, A., Gimeno, L., Nieto, R., Morán-Tejeda, E., Lorenzo-
17 Lacruz, J., Beguería, S., and Zabalza, J.: Effects of warming processes on droughts and water resources in the
18 NW Iberian Peninsula (1930-2006). *Climate Research*, 48(2-3), 203–212, 2011b.
- 19 Xu, J., Ren, L., Yu, Z., and Yuan, F.: Effects of the spatial resolution of digital elevation model data on the
20 performance of TOPMODEL. *IAHS-AISH Publication*, 311, 178–185, 2007.
- 21 Yang, G., He, X.L., Zheng, T.G., Maina, J.N., Li, J.F., and Liu, H.L.: Integrated agricultural irrigation
22 management technique in the arid inland area, China. *Journal of Food, Agriculture and Environment*, 10(1),
23 736–741, 2012.
- 24 Zhao, R., Chen, Y., Shi, P., Zhang, L., Pan, J., and Zhao, H.: Land use and land cover change and driving
25 mechanism in the arid inland river basin: a case study of Tarim River, Xinjiang, China. *Environmental Earth*
26 *Sciences*, 68(2), 591–604, 2013.
- 27

1 **Figure 1** Geographic situation of the Estaña catchment in NE Spain (a); map of soil types (b); picture of the
 2 study area showing the “*Estanque de Arriba*” lake and the crops located in the hillside and the lowlands of the
 3 catchment (c); monthly average (period 1997-2011) values of maximum rainfall intensity (I_{30}) and number of
 4 erosive rainfall events (d); annual values of precipitation recorded at the Canelles weather station for the period
 5 1941-2011 (e); and monthly average (period 1997-2011) rainfall (Canelles weather station), potential reference
 6 evapotranspiration and minimum and maximum temperature (Barbastro weather station) (f).

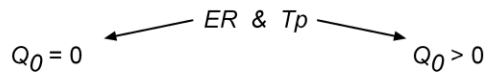


7
8
9

- 1 **Figure 2** Step-by-step procedures to estimate the actual available water (W_{aa}) at pixel scale (for more details, see
 2 López-Vicente and Navas, 2012 and López-Vicente et al., 2013).

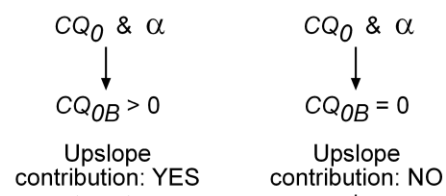
Step 1 (Q_0 map)

Characteristics:



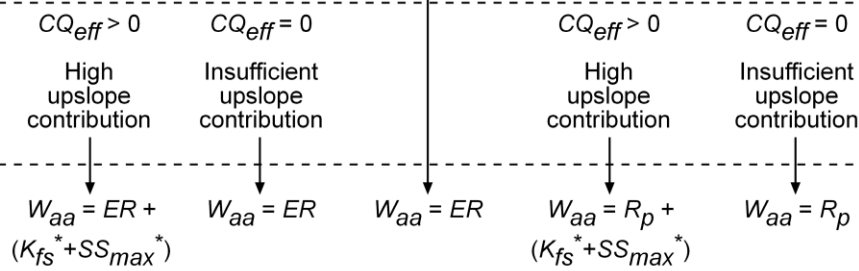
Step 2 (CQ_{0B} map)

Characteristics:



Step 3 (CQ_{eff} map)

Characteristics:



Situation:

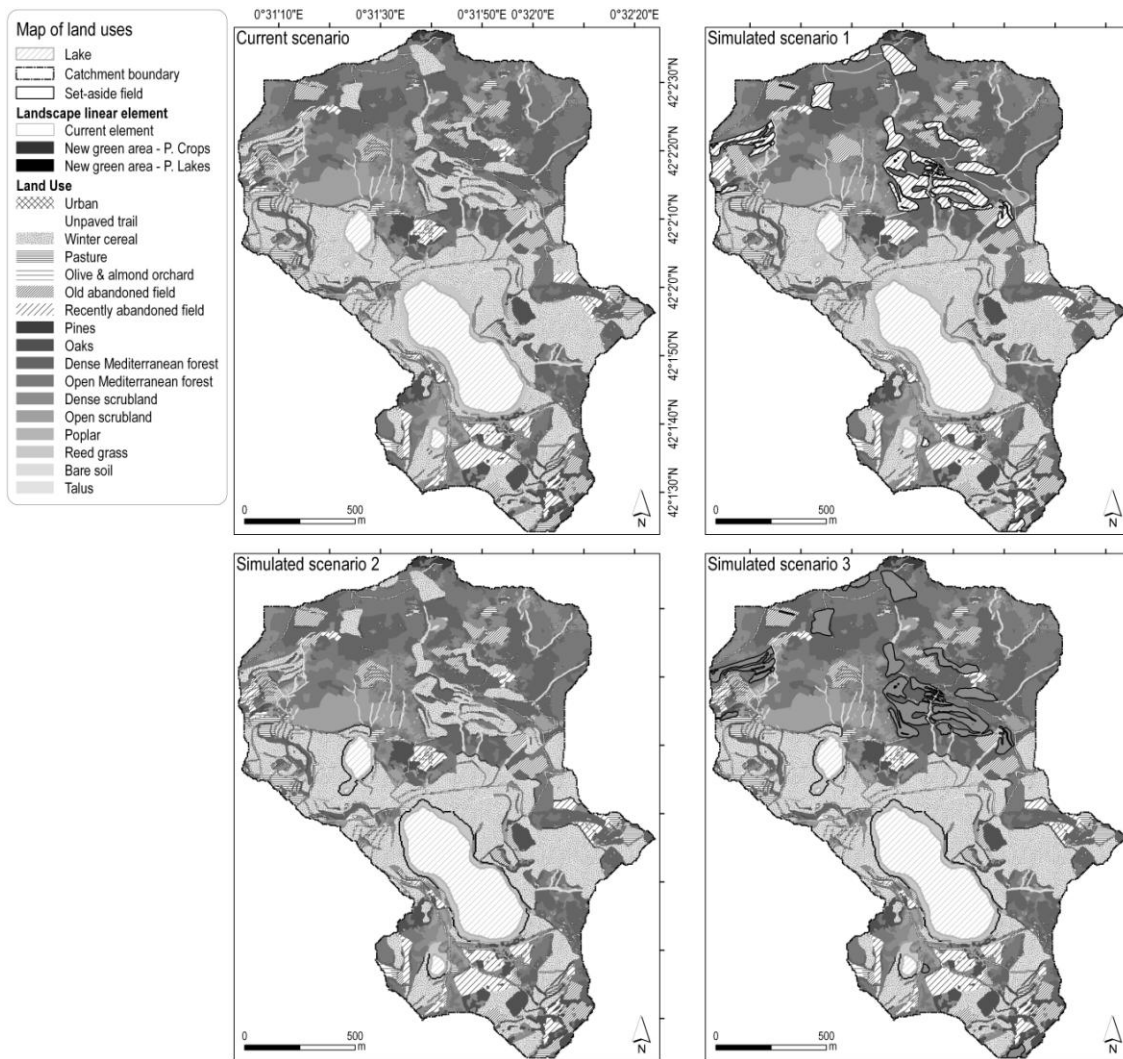
A B C D E

$W_{aa} = ER + (K_{fs}^* + SS_{max}^*)$ $W_{aa} = ER$ $W_{aa} = ER$ $W_{aa} = R_p + (K_{fs}^* + SS_{max}^*)$ $W_{aa} = R_p$

- 3
 4 ER : Effective rainfall; T_p : Time to ponding; Q_0 : potential runoff per raster cell; CQ_0 : potential cumulative
 5 runoff; α : water balance factor; CQ_{0B} : balanced potential cumulative runoff; CQ_{eff} : effective cumulative runoff;
 6 K_{fs}^* : saturated hydraulic conductivity ($K_{fs} T q_m e_m$, see Eq. (9)); SS_{max}^* : maximum surface storage capacity (SS_{max-m}
 7 e_m , see Eq. (9)); R_p : rainfall to ponding.

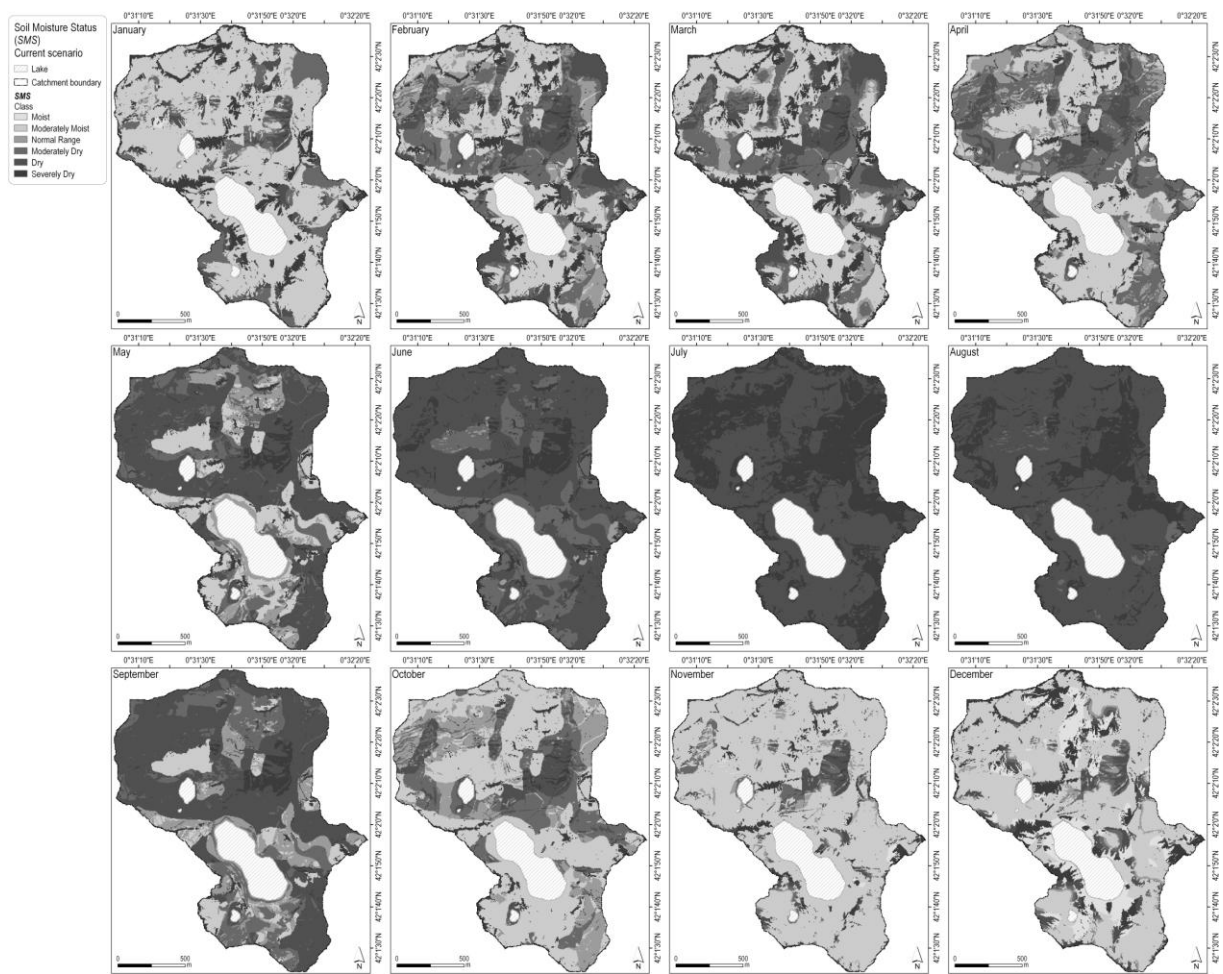
- 8
 9

1 **Figure 3** Maps of the different land use scenarios simulated in this study (see Material and Methods section for
 2 more details).



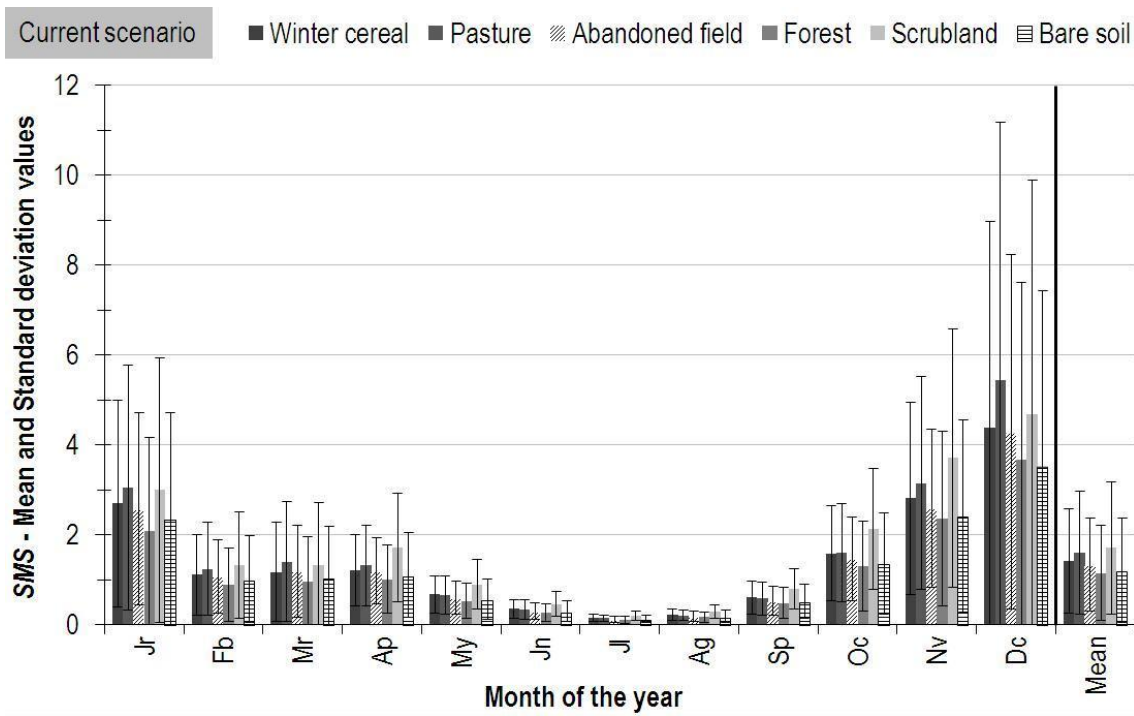
3
 4
 5

1 **Figure 4** Monthly maps of Soil Moisture Status in the Estaña catchment calculated for the current scenario of
2 land uses.



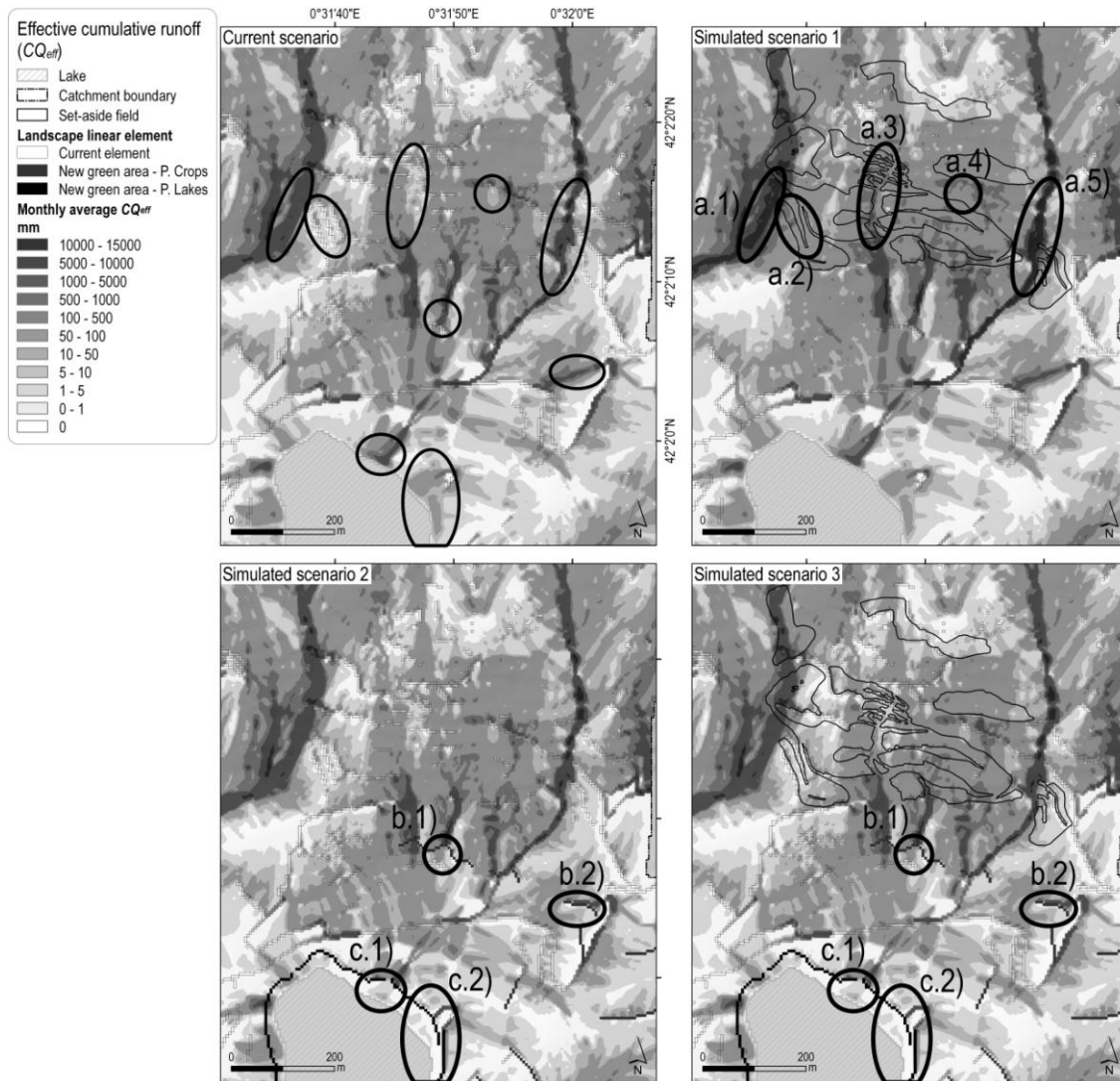
3
4
5

1 **Figure 5** Monthly values of Soil Moisture Status in the Estaña Lakes Catchment calculated for the main land
 2 uses under the current scenario.



3
 4
 5

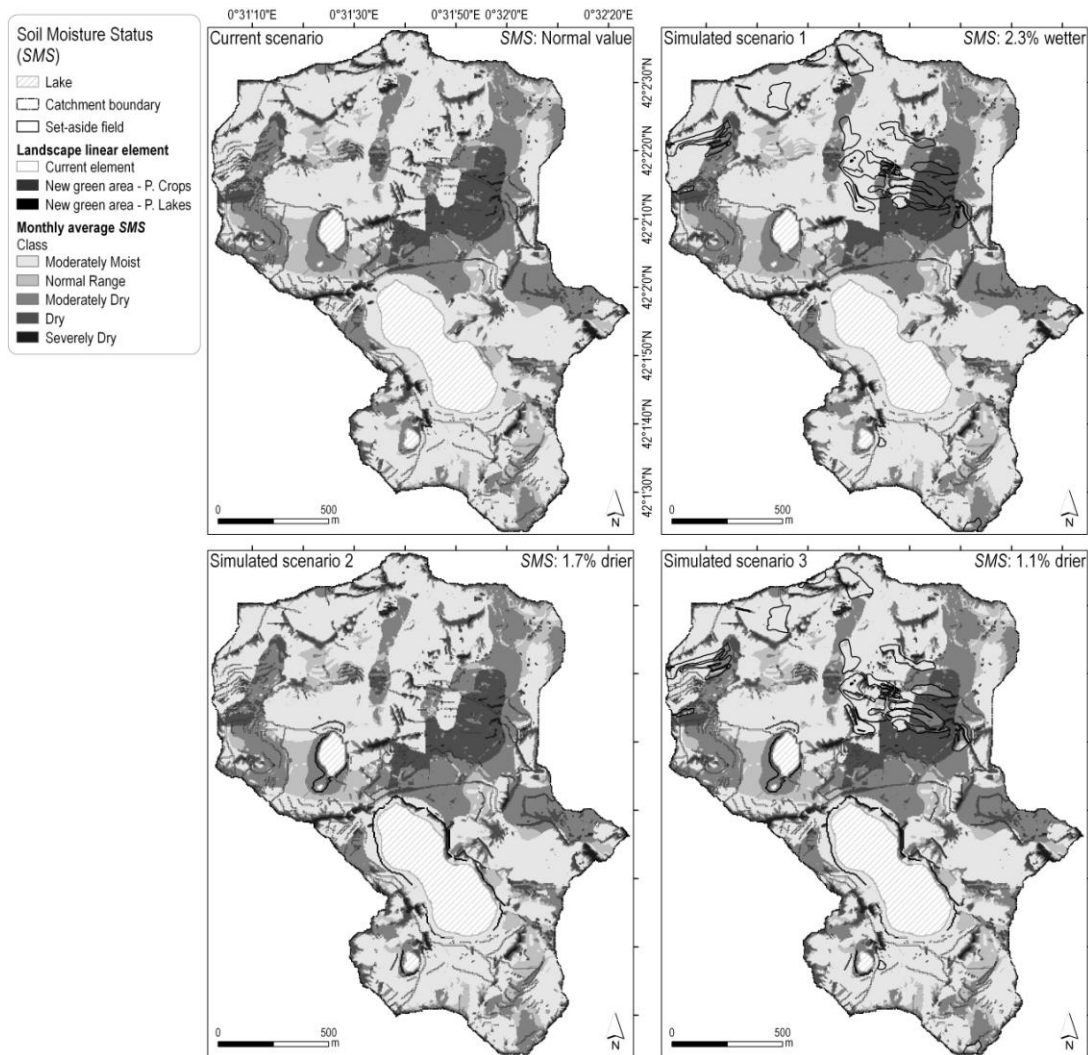
1 **Figure 6** Detailed maps of the effective cumulative runoff in the area surrounding the main overland flow path
 2 line generated in the four scenarios simulated in this study and in the area surrounding the northern part of the
 3 “*Estanque Grande de Abajo*” Lake.



4
 5 Legend: P. Crops: “green area” protecting the crops; P. Lakes: “green area” protecting the lakes.

6
 7

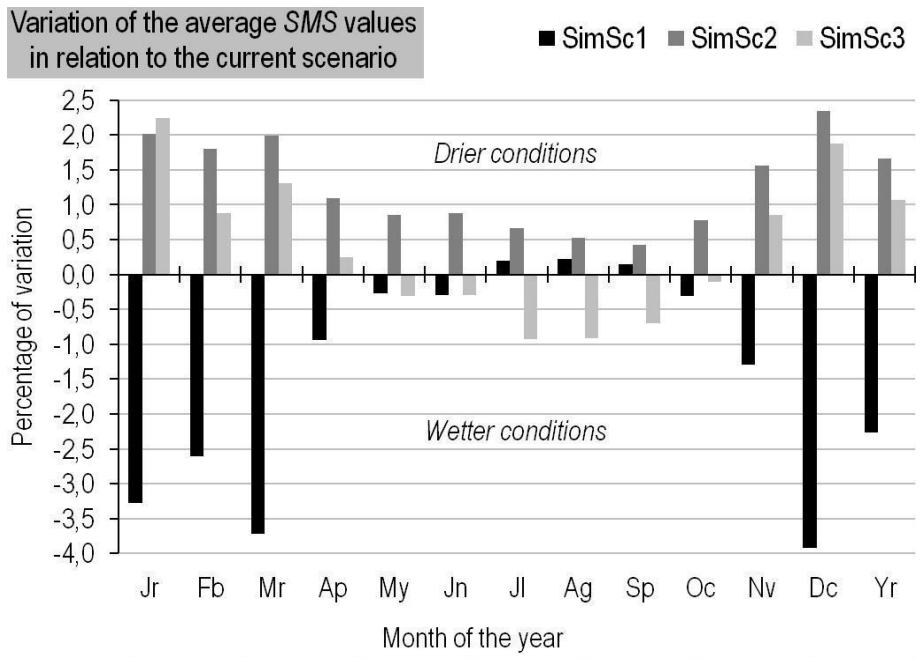
1 **Figure 7** Maps of average monthly Soil Moisture Status (SMS) for the current scenario and the three simulated
 2 land use scenarios in the Estaña Lakes catchment.



3
 4 Legend: P. Crops: “green area” protecting the crops; P. Lakes: “green area” protecting the lakes.

5
 6

1 **Figure 8** Percentage of variation of the monthly average values of Soil Moisture Status (SMS) in the Estaña
 2 Lake's Catchment for the three simulated scenarios in relation to the current scenario.



3
 4
 5

1 **Table 1** Classes for wet and dry conditions for the soil moisture status (SMS) of the DR2 model.

SMS value	Wetness-Drought index categories
≥ 100	Severely moist
10 to 100	Moist
1.1 to 10	Moderately moist
0.9 to 1.1	Normal range
0.5 to 0.9	Moderately dry
0.1 to 0.5	Dry
0 to 0.1	Severely dry

2

3

4 **Table 2** Landscape characteristics of the current and simulated scenarios in the Estaña Lake’s Catchment. The
 5 “Simulated scenario 1” represents the worse-case-scenario and the “Simulated scenario 2” and “Simulated
 6 scenario 3” includes the creation of “green areas” in accordance with the new Common Agricultural Policy of
 7 the European Union (draft of the proposal presented in Brussels in October 2011;
 8 http://ec.europa.eu/agriculture/cap-post-2013/legal-proposals/index_en.htm).

Landscape characteristics	Current scenario	Simulated scenario 1	Simulated scenario 2	Simulated scenario 3
New set-aside fields	No	Yes	No	Yes
Landscape linear elements associated with the set-aside fields	No change	Dismantled	No change	Preserved
SUPPORT PRACTICES				
- Revegetation of the set-aside fields with shrubs	No	No	No	Yes
- New “green areas” protecting the fields located in gentle areas	No	No	Yes	Yes
- New “green areas” protecting the lakes	No	No	Yes	Yes

9